



Unexpected Bisboronic Dicationic Acid Obtained from One-Pot Condensation Reaction of 3-Aminophenylboronic Acid and 2,6-Pyridincarboxyaldehyde

Arturo González-hernández, Jacobo Rivera-segura, Pascal G. Lacroix, Victor Barba

► To cite this version:

Arturo González-hernández, Jacobo Rivera-segura, Pascal G. Lacroix, Victor Barba. Unexpected Bisboronic Dicationic Acid Obtained from One-Pot Condensation Reaction of 3-Aminophenylboronic Acid and 2,6-Pyridincarboxyaldehyde. *ChemistrySelect*, 2019, 4 (30), pp.8822-8828. <10.1002/slct.201900302>. <hal-02350510>

HAL Id: hal-02350510

<https://hal.science/hal-02350510v1>

Submitted on 4 Nov 2020

HAL is a multi-disciplinary open access archive for the deposit and dissemination of scientific research documents, whether they are published or not. The documents may come from teaching and research institutions in France or abroad, or from public or private research centers.

L'archive ouverte pluridisciplinaire **HAL**, est destinée au dépôt et à la diffusion de documents scientifiques de niveau recherche, publiés ou non, émanant des établissements d'enseignement et de recherche français ou étrangers, des laboratoires publics ou privés.



HAL Authorization

Unexpected *Bisboronic Dicationic Acid* Obtained from One- Pot Condensation Reaction of 3- Aminophenylboronic Acid and 2,6- Pyridincarboxyaldehyde

Arturo González-Hernández,^a Jacobo Rivera-Segura,^a Pascal G. Lacroix,^b and Victor Barba.^{a*}

^aCentro de Investigaciones Químicas-IICBA. *Universidad Autónoma del Estado de Morelos*. Av. Universidad 1001. Col. Chamilpa, Cuernavaca Morelos C.P 62209.

^bCNRS, LCC (Laboratoire de Chimie de Coordination), 205, Route de Narbonne, Toulouse F-31077, France

Keywords: *Boronic acids, condensation reaction, anion exchange, building block, syn-anti isomerization.*

Abstract: A double condensation reaction between 3-aminophenylboronic acid monohydrate and 2,6-pyridincarboxyaldehyde forms the bisboronic acid (**1**), the reaction was carried out in methanol with the presence of sulfuric acid as catalyst. The product contains a delocalized dicationic moiety related to the cyclopent(hi)aceanthrylene group including methylsulfate ($\text{CH}_3\text{OSO}_3^-$) as anion (**1a**). Treatment with CaCl_2 under heating produces the anion interchange leading the chloride as anion (**1b**). Both salts were crystallized by slow solvent diffusion and the X-ray diffraction analysis reveals the presence of $\text{O-H}\cdots\text{O}$ hydrogen bonds favoring the 2D supramolecular arrangements. Three different motives were formed for **1a** with the participation of water molecules, the methylsulfate anion and the boronic acid groups; by the way for **1b**, the chloride anion interacts with a BOH group, a methanol molecule and has an electrostatic interaction with a cationic five membered ring. The possibility for *syn-anti* isomerization at room temperature is confirmed by computations with a weak energy barrier of $17.7 \text{ kcal mol}^{-1}$.

Corresponding author: Tel/fax +52 777 3297997.

E-mail: vbarba@uaem.mx

Introduction

Boronic acids have attracted the attention since the mid-19th century, because of their relatively straightforward preparation and chemical versatility. Preparation of substituted alkyl- or aryl boronic acid derivatives is relevant for its wide applications in three main areas: organic synthesis,^[1] sensing and separation,^[2] and building blocks in the preparation of well-structured organic molecules.^[3] Initially, the preparation of boronic acids was carried out mainly by hydrolysis of alkyl- or arylboranes. Nonetheless, additional approaches have been developed to prepare boronic acids including transmetallation, metal-halogen exchange, direct boronylation by transition metal-catalyzed and coupling of diboronyl species with aryl halides.^[4] Essentially, modifications of the organic fragments attached to the boronic moieties by simple synthetic procedures are important methods to get aryl- or alkyl-boronic acids in an easy way.

Since the presence of $B(OH)_2$ groups, boronic acids are able to react in different ways. Dehydration under heating leads to the highly stable six-membered boroxines by self-condensation reaction. Thus, self-condensing of more than two boronic acid groups included at the same molecule with the adequate geometry, leads to interesting covalent 2D and 3D organic frameworks.^[5-7] Furthermore, the most investigated reaction condensation involving boronic acids occurs with alcohol substrates forming boronic esters; essentially, reaction with 1,2-, and 1,3-diols generate five and six membered rings which are relevant to covalent organic frameworks (COFs) formation, and indeed several reviews had account for the development of COFs chemistry.^[8-11] The proper geometry selection of the bis- or tris-diols with mono-, di- or tri- boronic acids, results in the modulation of geometry and size of the synthesized 2D derivatives as macrocycles^[12,13] or polymeric derivatives,^[14-16] and 3D compounds as cages,^[17-19] capsules^[20] and COFs.^[21,22] Cavitand compounds have been applied as molecular receptors and used for small molecules recognition.^[23-25]

The ability for reversible binding with 1,2- and 1,3- diols of $B(OH)_2$ groups, has also been focused on development of chemosensors for detection of saccharides.^[26-28] In boronic acid based sensing systems, the boronic acid group acts as a receptor. Such research has been oriented to glucose detection,^[29,30] in which the recognition process is monitored using

UV-vis or fluorescence spectroscopy. Along this line, bisboronic dicationic acids derived from pyridium fragments have been used for glucose detection using viologen as a quencher.^[31-33] In fact, a variety of chromophores and fluorophores have been coupled to boronic acids in order to increase the detection ability,^[34] allowing the molecular recognition of biochemically active molecules.^[35,36] The B(OH)₂ groups also contribute to the recognition process by means of hydrogen bonding wherein supramolecular arrangements structurally well established are obtained.^[37] For instance, diboronic acids in combination with bipyridine forms 2D structures engineered through O-H...N and C-H...O motifs.^[38-40]

In the present report, an unexpected double condensation reaction between 2,6-pyridinecarboxyaldehyde with 3-aminophenylboronic acid yields a bisboronic dicationic acid having methylsulfate as anion (**1a**), anion exchange was observed by treatment with CaCl₂ (**1b**), molecular structures were corroborated by X-ray diffraction analysis and DFT computational analysis reveals the presence *syn-anti* isomers.

Results and discussion

The equimolar condensation reaction of 2,6-pyridinecarboxyaldehyde with 3-aminophenylboronic acid monohydrate in methanol, offered the diboronic compound 1,7b,10c,6-tetraazacyclopenta[hi]aceanthrylene-1,6-diium-bis(3-phenylboronic) acid (**1a**) in moderate yield (Scheme 1). The reaction required the addition of some drops of sulfuric acid and 6 h of reflux. Product **1a** was obtained as a red dark solid, stable under moisture at room temperature, well soluble in polar organic solvents with high melting point observed at T > 350°C.

Compound **1a** was obtained as a dicationic molecule having two CH₃OSO₃⁻ anions coming from the use of sulfuric acid as catalyst together the methanolysis process. The intense red color is attributed to the presence of the five heterocycles fused system in the π -conjugated central core (like a cyclopent(hi)aceanthrylene group). Three resonant forms are possible for delocalized core (**I-III**, Scheme 2), for which the positive charges are located either on the nitrogen atoms on the periphery (**I-II**), or on the internal nitrogen atoms (**III**). Computations were performed at the Density Functional Theory (DFT) level to establish

which structure corresponds to the main contribution at equilibrium, nevertheless the energy of the distribution charge was similar for the three species and no real difference was found.

The IR spectrum showed an intense broad band located at 3306 cm^{-1} assigned to the $\nu(\text{O-H})$ groups. In addition, a thin band at 1644 cm^{-1} was assigned to the stretching band of the C=N moieties.

The analysis of the ^1H NMR spectrum of **1a** revealed the C_2 symmetry for this molecule showing signals for only one half of the molecule. The proton of the five membered ring heterocycle (H-7) was shifted to $\delta = 8.02\text{ ppm}$. Signal for OH groups was observed at lowest field ($\delta = 8.50\text{ ppm}$) and signal for proton located between the boron and nitrogen moieties (H-2) is shifted to $\delta = 8.34\text{ ppm}$ as a singlet. At ^{13}C NMR, signals for carbons atoms of the five membered heterocycle were shifted to $\delta = 131.2, 131.7$ and 133.4 ppm for C-7, C-8 and 13, respectively. 2D NMR spectra as COSY, HETCOR and HSQC allows a complete elucidation for this compound. Signal for ^{11}B NMR was observed at $\delta = 32\text{ ppm}$ corresponding to a tricoordinated specie.

Suitable crystals for X- ray diffraction analysis were obtained by slow diffusion of a methanol concentrate solution. Compound **1a** crystallized in the triclinic crystal system (space group P-1). A diboronic molecule, four water molecules and two $\text{CH}_3\text{OSO}_3^-$ anions are present at the unit cell. The molecular structure of **1a** is illustrated at Figure 1, in which water molecules and anions are excluded for clarity. Selected crystallographic data are showed at Table 1 and selected bond distances and angles are showed at Table 2. Compound **1a** belongs to the S_2 symmetry group, wherein the two boronic acid groups are in *anti*-relationship. The torsion angles C2-C3-N1-C13 and C4-C3-N1-C13 with values of $80.9(2)^\circ$ and $99.1(2)^\circ$, respectively, reveals the orthogonal position respect to the central five heterocycles core. Nonetheless, the boronic acid groups are coplanar within the aromatic rings in which are attached, torsion angle value for O2-B1-C1-C2 is only $4.6(3)^\circ$. Atoms at main core are in a planar geometry as observed from the angles values that in most cases are close to 120° , in fact the torsion angle value for N1-C13-C12'-C11' of $3.5(2)^\circ$ describes the slow deviation from planarity. The smaller angles are registered for

the five membered ring heterocycle with values from 105.80(15) to 110.02 (14)°. Largest values corresponds to angles C7-C8-C9 (135.98(17))°, N1-C13-C12' (131.57(15))° and C11-C12.C13' (130.81(16))°. Cyclic N-C distances are in the range from 1.343(12) to 1.395(2) Å, meanwhile exocyclic N-C distance is longer (N1-C3 1.453(2) Å).

The presence of water molecules as well as the (CH₃OSO₃⁻) anion give rise to hydrogen bond interactions stabilizing the supramolecular network. Three different motifs are observed including for all of them four O-H...O hydrogen bonds with distances of 1.925 to 2.104 Å. **I**) a twelve membered ring is formed by the interaction of four OH groups from two boronic moieties and two water molecules. **II**) a ten membered ring is formed by the interaction of two water molecules, a OH group from a boronic moiety and two oxygen atoms from a methylsulfate anion. **III**) a twelve membered ring is formed by interaction of two water molecules and the two methylsulfate anions (Figure 2). The motif **I** give place to stair conformations at supramolecular level in which two water molecules connect two boronic acid groups as depicted at Figure 3.

As observable from the X ray analysis, the structure showed that the boronic acid moieties are in *anti* conformation, nevertheless the *syn* isomer having the boronic acids oriented at the same side could be envisioned (Figure 4-top). The two conformations were computed by DFT. The optimization of the geometries reveals that the most stable isomer is the *anti*-. Nevertheless, the energy difference between both *syn*- and *anti*- species is only 0.1 kcal mol⁻¹. Moreover, the energy barrier in the *anti* ⇌ *syn* isomerization, shown in Figure 4-bottom, indicates a possibility for free rotation at room temperature, with an energy barrier of 17.7 kcal mol⁻¹. Therefore, it is not possible to isolate a single form and the experimental NMR as well as UV-vis spectra should arise from the contribution of both *syn*- and *anti*- components present in the mixture.

The UV-vis spectrum obtained in methanol solution at 10⁻⁵ M reveals five bands at 221, 274, 410, 432 and 462 nm attributed to π-π* and n-π* transitions. By the way, fluorescent properties were established by the excitation spectrum which shown an intense band at 364 nm Figure 5. The dominant (1→3) electronic transitions computed for the *syn*- and *anti*-

derivatives are compared to the experimental UV-vis spectrum in Table 3. The computed data indicate that the spectrum of each *syn*- and *anti*- isomer arise from a single low-lying transition, which apparently strikes with the experimental UV-vis spectrum, where bands are observed at 462 nm and 432 nm, together with a poorly defined signal of lower intensity, at around 410 nm. Nevertheless, assuming a 1/1 mixture of both species in solution, the agreement between experiment and computation is excellent for the two intense transitions, which allows the analysis of the computed transitions to be carried out more precisely.

Details of the dominant transition contributing to the *syn*- and *anti*- spectra are provided in Table 4. The data reveal two closely related spectra with a highly dominant HOMO → LUMO based transition. The only noticeable effects occurring during the *anti*-/ *syn*- isomerization process is a slight blue shift and reduced intensity in the *cis*- isomer, which is fully confirmed by the experimental spectrum. The orbitals of interest are shown in Figure 6. Both HOMO and LUMO levels appear strongly located on the rigid central π -conjugated structure, and therefore are basically the same. While the four nitrogen atoms of the skeleton do not contribute to the HOMO level, the presence of electron density on the external nitrogen connected to the phenyl-B(OH)₂ substituents seems to indicate that the dominant Lewis structures correspond to that illustrated in Scheme 2 as **I** and **II**.

Compound **1a** was treated with an excess of CaCl₂ in a methanol/benzene solvent. After 4 h under reflux, the solution was concentrated by solvent evaporation. Slow cooling/evaporation solvent allowed obtaining reddish crystals suitable for X-ray diffraction analysis. Structure refinement indicates the partial esterification of the boronic acid, an OH group being replaced by a MeO group derived from a methanolysis reaction (Figure 1, **1b**). Nevertheless, the most noticeable change is the anion exchange, CH₃OSO₃⁻ being replaced by Cl⁻. Thus at unit cell one dicationic molecule, two chloride ions and two methanol solvent molecules are present. Chloride anion is engaged in three strong secondary interactions at least: a hydrogen bond with the B-OH group (BO-H...Cl bond distance of 2.368 Å), a shorter hydrogen bond with the methanol molecule (MeO-H...Cl bond distance of 2.305 Å), and finally one electrostatic interaction with the positively

charged five membered ring ($\text{Cl} \cdots \pi_{\text{five membered center ring}}$ distance of 3.318 Å). These intermolecular contacts give rise to the formation of 1D polymeric chains, while self-assembly of several chains leads to a supramolecular arrangement as depicted at Figure 7.

Conclusions

The simple double condensation reaction between two equivalents of 2,6-pyridinecarboxyaldehyde and 3-aminophenylboronic acid monohydrate affords a fluorescent bisboronic acid, in moderate yield. This product consists in a dicationic specie having a central π -conjugated core, with the two boronic acid groups in *anti*-disposition. DFT calculations show that the *syn* isomer exists at room temperature with a possibility for *syn-anti*- isomerization. Treatment with CaCl_2 offers anion exchange and partial esterification of the boronic group. The synthesis of this new bisboronic dicationic acid compound, opens the possibility to construct a new variety of compounds with interesting photophysical properties and, constitutes a remarkable building block in self-assembly processes.

Experimental Part

Materials

All reagents and solvents were acquired from commercial suppliers and used without further purification.

Instrumentation

The ^1H , ^{13}C and ^{11}B NMR were recorded at room temperature using a Varian Unit 400 spectrophotometer. As standard references was used TMS (internal, ^1H , $\delta = 0.00$ ppm, ^{13}C , $\delta = 0.0$ ppm) and $\text{BF}_3 \cdot \text{Et}_2\text{O}$ (external, ^{11}B , $\delta = 0.0$ ppm). 2D COSY and HETCOR experiments have been carried out for the unambiguous assignment of the ^1H and ^{13}C NMR spectra. All chemical shifts are stated in ppm and coupling constants are reported in Hz. Assignments for ^1H and ^{13}C NMR spectra are in according to the X-ray numbering (Figure 1). Infrared spectra have been recorded on a Bruker Vector 22 FT-IR spectrophotometer.

Mass spectra were obtained with MStation JMS-700 JEOL equipment. Melting points were determined with a Büchi Pion B-540 digital apparatus. The electronic absorption spectra were recorded at 25 °C on a Genesys 10S spectrophotometer.

X-ray crystal-structure determination

Intensity data for compounds **1a** and **1b** were collected at T= 100 K with Cu-K α radiation (λ = 1.54184 Å), monochromator: graphite on an Agilent Technologies SuperNova diffractometer equipped with the EOsS2 CCD area detector and an Oxford Instruments Cryogen cooler. Crystal data, data collection parameters and convergence results are listed in Table 1. The measured intensities were reduced to F^2 and corrected for absorption using spherical harmonics (CryAlisPro).^[41] Intensities were corrected for Lorentz and polarization effects. Structure solution, refinement, and data output were performed with the OLEX2 program package^[42] using SHELXL-2014^[43] for the refinement. Non-hydrogen atoms were refined anisotropically. All hydrogen atoms were placed in geometrically calculated positions using the riding model. Intermolecular distances were analyzed with MERCURY.^[44]

Computational methods

The molecular geometries of the *syn*- and *anti*- isomers of the bis boronated compound were fully optimized using the Gaussian-09 program package^[45] within the framework of the DFT at the B3LYP/6-31G* level. B3LYP^[46,47] was selected as a widely used method for computations of organic molecules in addition with its accuracy to reproduce the present experimental data. Vibrational analysis was performed at the same level to verify that the stationary point corresponded to minima on the potential energy surfaces. Solvent effect were included using the polarizable continuum model (PCM) implemented in Gaussain09 for methanol (ϵ = 32.613). For the *anti* derivative, the computed geometry was found to be centrosymmetric, within a tolerance of 0.0005 Å. The actual structure was therefore assumed to be centrosymmetric. The scan for the *anti* \rightleftharpoons *syn* isomerization was

carried out by steps of 5°. The rotation angle was defined as the torsion angle between the rigid central molecular skeleton and the phenyl ring and was introduced in the computation as the C(4)-C(3)-N(1)-C(7) torsion within the ModRedundant keyword used in Gaussian09. The UV-vis electronic spectra were computed at the same B3LYP/6-31G* level. Molecular orbitals were using GABEDIT.^[48]

General method for the preparation of boronic acid 1a

Compound **1a** was synthesized from the equimolecular reaction of the corresponding 2,6-pyridinecarboxialdehyde (0.043 g, 0.12 mmol) with 3-aminophenylboronic acid monohydrate (0.10 g, 0.12 mmol), using 40 mL of methanol and three drops of sulfuric acid as a catalyst. The reaction mixture was stirred for 6 h under reflux. After that, part of the solvent was removed using a Dean-Stark trap and cooling then 60 mL of hexane was adding and left the solution until evaporation. The oil was washed with methanol (3 x 10 mL) to recover the final product. The product was obtained as red dark powder. Yield: (26%); m.p. > 350°C. IR (KBr) ν (cm⁻¹): 3306 (OH) (w), 3098 (w), 1644 (C=N) (m), 1515 (w), 1428(m), 1362 (m), 1310 (w), 1215(m), 1065 (m), 998(s), 795 (w), 760 (s), 698 (s), 672 (m), 637 (m). MS (FAB⁺) m/z (%): 492 (15) [$M^+ \cdot H_2O - (2CH_3OSO_3)$], 237 (19) [m/z]. ¹H NMR (400 MHz, DMSO-d₆) δ : 8.50 (4H, br, s, OH), 8.34 (2H, s, H-2), 8.22 (2H, t, J = 4.8 Hz, H-10), 8.02 (2H, s, H-7), 7.79 (4H, d, J = 4.8 Hz, H-9, H-11), 7.41 (2H, d, J = 8.00 Hz, H-6), 6.83 (2H, t, J = 8.00 Hz, H-5), 5.57 (2H, d, J = 8.00 Hz, H-4). ¹³C NMR (100 MHz, DMSO-d₆) δ : 138.34 (C-1), 138.2 (C-10), 133.4 (C-13), 131.7 (C-8), 131.2 (C-7), 130.7 (C-9), 129.4 (C-5), 127.7 (C-12), 127.6 (C-11), 124.5 (C-3), 121.3 (C-2, C-6), 113.6 (C-4). ¹¹B NMR (128.17 MHz, DMSO-d₆) δ : 32 ppm ($h_{1/2}$ = 1100 Hz).

Supplementary information

CCDC Nos. 1874948 and 1874949 contain the supplementary crystallographic data for **1a** and **1b**, respectively. These data can be obtained free of charge from The Cambridge Crystallographic Data Centre via www.ccdc.cam.ac.uk/data_request/cif.

Acknowledgements

The authors thank Consejo Nacional de Ciencia y Tecnología (CONACyT) for financial support, project 157743. Arturo Hernandez Gonzalez acknowledges fellowship 170443 from CONACYT. The work was performed within the French-Mexican International Associated Laboratory (LIA-LCMMC).

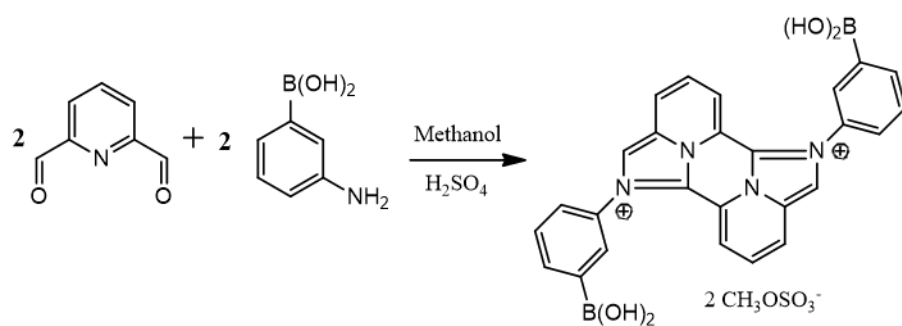
References

- [1] N. Miyaura, A. Suzuki, *Chem. Rev.* **1995**, 95, 2457-2483.
- [2] R. Nishiyabu, Y. Kubo, T.D. James, J. S. Fossey, *Chem. Commun.* **2011**, 47, 1106-1123.
- [3] R. Nishiyabu, Y. Kubo, T.D. James, J. S. Fossey, *Chem. Commun.* **2011**, 47, 1124-1150.
- [4] Hall D.G. Boronic acids; Wiley-VCH Verlag GmbH & Co KGaA: Weinheim, Germany, **2011**; Chapter 1.
- [5] Y. Li, J. Ding, M. Day, Y. Tao, J. Lu, M. D'Iorio, *Chem. Mater.* **2003**, 15, 4936-4943.
- [6] S. Helten, B. Sahoo, V. Bon, I. Senkovska, S. Kaskel, F. Glorius, *Cryst. Eng. Comm.* **2015**, 17, 307-312.
- [7] K. Ono, K. Johmoto, N. Yasuda, H. Uekusa, S. Fujii, M. Kiguchi, N. Iwasawa, *J. Am. Chem. Soc.* **2015**, 137, 7015-7018.
- [8] Kay Severin, *Dalton Trans.* **2009**, 5254-5264.
- [9] N. Fujita, S. Shinkai, T. D. James, *Chem. Asian J.* **2008**, 3, 1076-1091.
- [10] Y. Kubo, R. Nishiyabua, T. D. James, *Chem. Commun.* **2015**, 51, 2005-2020.
- [11] S. L. Huang, G. X. Jin, H. K. Luo, T. S. A. Hor, *Chem. Asian J.* **2015**, 10, 24-42.
- [12] S. Ito, K. Ono, N. Iwasawa, *J. Am. Chem. Soc.* **2012**, 134, 13962-13965.
- [13] N. A. Celis, C. Godoy-Alcántar, J. Guerrero-Álvarez, V. Barba, *Eur. J. Inorg. Chem.* **2014**, 1477-1484.
- [14] Y. Matsushima, R. Nishiyabu, N. Takanashi, M. Haruta, H. Kimura, Y. Kubo, *J. Mater. Chem.* **2012**, 22, 24124-24131.
- [15] T. Y. Zhou, F. Lin, Z. T. Li, X. Zhao, *Macromolecules.* **2013**, 46, 7745-7752.
- [16] E. L. Spitler, B. T. Koo, J. L. Novotney, J. W. Colson, F. J. Uribe-Romo, G. D. Gutierrez, P. Clancy, W. R. Dichtel, *J. Am. Chem. Soc.* **2011**, 133, 19416-19421.
- [17] A. Dhara and F. Beuerle, *Chem. Eur. J.* **2015**, 21, 1-7.
- [18] S. Klotzbach, T. Scherpf, F. Beuerle, *Chem. Commun.* **2014**, 50, 12454-12457.
- [19] S. Klotzbach, F. Beuerle, *Angew. Chem. Int. Ed.* **2015**, 54, 10356-10360.
- [20] N. Nishimura, K. Kobayashi, *J. Org. Chem.* **2010**, 75, 6079-6085.
- [21] H. M. El-Kaderi, J. R. Hunt, J. L. Mendoza-Cortes, A. P. Cote, R. E. Taylor, M. OPKeeffe, O. M. Yaghi, *Science.* **2007**, 316, 268-272.

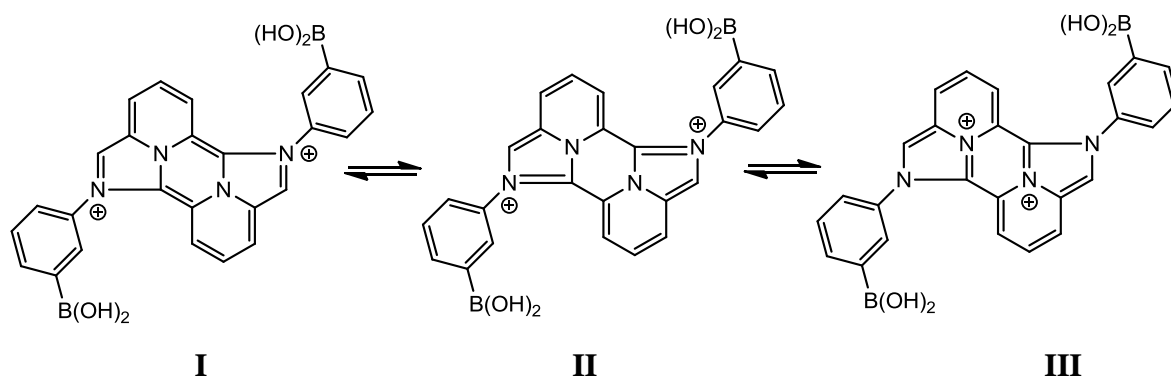
- [22] A. P. Cote, A. I. Benin, N. W. Ockwig, M. OPKeeffe, A. J. Matzger, O. M. Yaghi, *Science* **2005**, *310*, 1166-1170.
- [23] S. D. Bull, M. G. Davidson, J. M. H. Van den Elsen, J. S. Fossey, A. T. A. Jenkins, Y. B. Jiang, Y. Kubo, F. Marken, K. Sakurai, J. Zhao, T. D. James, *Acc. Chem. Res.* **2013**, *46*, 312-326.
- [24] K. Kataoka, S. Okuyama, T. Minami, T. D. James, Y. Kubo, *Chem. Commun.* **2009**, 1682-1684.
- [25] N. Iwasawa, H. Takahagi, K. Ono, K. Fujii, H. Uekusa, *Chem. Commun.* **2012**, *48*, 7477-7479.
- [26] S. Arimori, H. Murakami, M. Takeuchi, S. Shinkai, *J. Chem. Soc., Chem. Commun.* **1995**, 961-962.
- [27] R. Badugu, J. R. Lakowicz, C. D. Geddes, *Bioorg. Med. Chem.* **2005**, *13*, 113-119.
- [28] J. S. Hansena, M. Fickera, J. F. Petersena, J. B. Christensena, T. Hoeg-Jensen, *Tet. Lett.* **2013**, *54*, 1849-1852.
- [29] Y. J. Huang, W. J. Ouyang, X. Wu, Z. Li, J. S. Fossey, T. D. James, Y. B. Jiang, *J. Am. Chem. Soc.* **2013**, *135*, 1700-1703.
- [30] Z. Wanga, H. Leib, L. Feng, *Spectrochim. Acta A Mol. Biomol. Spectrosc.* **2013**, *114*, 293-297.
- [31] Z. Sharrett, S. Gamsey, J. Fat, D. Cunningham-Bryant, R. A. Wessling, B. Singaram, *Tet. Lett.* **2007**, *48*, 5125-5129.
- [32] J. N. Camara, J. T. Suri, F. E. Cappuccio, R. A. Wessling, B. Singaram, *Tet. Lett.* **2002**, *43*, 1139-1141.
- [33] S. Gamsey, N. A. Baxter, Z. Sharrett, D. B. Cordes, M. M. Olmstead, R. A. Wesslinga, B. Singaram, *Tetrahedron*, **2006**, *62*, 6321-6331.
- [34] D. Amilan-Jose, M. Elstner, A. Schiller, *Chem. Eur. J.* **2013**, *19*, 14451-14457.
- [35] J. Dong, S. Li, H. Wang, Q. Meng, L. Fan, H. Xie, C. Cao, W. Zhang, *Anal. Chem.* **2013**, *85*, 5884-5891.
- [36] W. L. A. Brooks, B. S. Sumerlin, *Chem. Rev.* **2016**, *116*, 1375-1397.
- [37] S. SeethaLekshmi, S. Varughese, L. Giri, V. R. Pedireddi, *Cryst. Growth Des.* **2014**, *14*, 4143-4154.
- [38] V. R. Pedireddi, N. SeethaLekshmi, *Tet. Lett.* **2004**, *45*, 1903-1906.
- [39] P. Rodriguez-Cuamatzi, R. Luna-Garcia, A. Torres-Huerta, M. I. Bernal-Uruchurtu, V. Barba, H. Höpfl, *Cryst. Growth Des.* **2009**, *9*, 1575-1583.
- [40] P. Sanchez-Portillo, V. Barba, *Chemistry Select.* **2017**, *2*, 11265-11272.
- [41] Agilent Technologies, CrysAlisPro, Version 1.171.37.35. Yarnton, Oxfordshire, United Kindom, **2014**.
- [42] O.V. Dolomanov, L.J. Bourhis, R.J. Gildea, J.A.K. Howard, H. Puschmann, *J. Appl. Cryst.* **2009**, *42*, 339-341.
- [43] G.M. Sheldrick, *Acta Crystallogr C.* **2015**, *71*, 3-8.
- [44] C.F. Macrae, P.R. Edgington, P. McCabe, E. Pidcock, G.P. Shields, R. Taylor, M. Towler, J. van de Streek, *J. Appl. Cryst.* **2006**, *39*, 453-457.

- [45] M. J. Frisch, G. W. Trucks, H. B. Schlegel, G. E. Scuseria, M. A. Robb, J. R. Cheeseman, G. Scalmani, V. Barone, B. Mennucci, G.A.Petersson, H. Nakatsuji, M. Caricato, X. Li, H. P. Hratchian, A. F. Izmaylov, J. Bloino, G. Zheng, J. L. Sonnenberg, M. Hada, M. Ehara, K. Toyota, R. Fukuda, J. Hasegawa, M. Ishida, T. Nakajima, Y. Honda, O. Kitao, H. Nakai, T. Vreven, Jr. J. A. Montgomery, J. E. Peralta, F. Ogliaro, M. Bearpark, J. J. Heyd, E. Brothers, K. N. Kudin, V. N. Staroverov, R. Kobayashi, J. Normand, K. Raghavachari, A. Rendell, J.C. Burant, S. S. Iyengar, J. Tomasi, M. Cossi, N. Rega, M. J. Millam, M. Klene, J. E. Knox, J. B. Cross, V. Bakken, C. Adamo, J. Jaramillo, R. Gomperts, R. E. Stratmann, O. Yazyev, A.J. Austin, R. Cammi, C. Pomelli, J. W. Ochterski, R. L. Martin, K. Morokuma, V. G. Zakrzewski, G. A. Voth, P. Salvador, J. J. Dannenberg, S. Dapprich, A. D. Daniels, Ö. Farkas, J. B. Foresman, J. V. Ortiz, J. Cioslowski, D. J. Fox, **2009**. Gaussian 09, Revision B.01, Gaussian Inc., Wallingford, CT.
- [46] A.D. Becke, *J. Chem. Phys.* **1993**, 98, 5648-5652.
- [47] P.J. Stephens, F.J. Devlin, C.F. Chabalowski, M.J. Frisch, *J. Phys. Chem.* **1994**, 98, 11623-11627.
- [48] A.R. Allouche, *J. Comput. Chem.* **2011**, 32, 174-182.

Figure Captions



Scheme 1. Synthesis of diboronic acid **1a**.



Scheme 2. Possible tautomeric dicationic species **I-III** presents for **1a**.

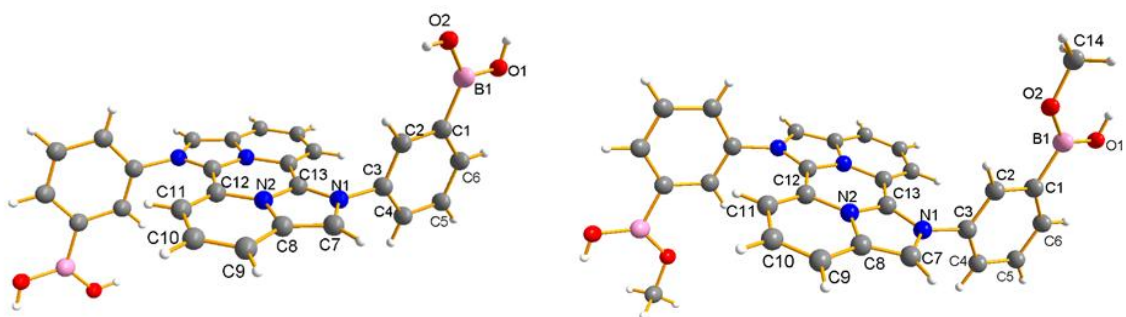


Figure 1. Molecular structures of compounds **1a** (left) and **1b** (right). Anions were excluded for a better visualization.

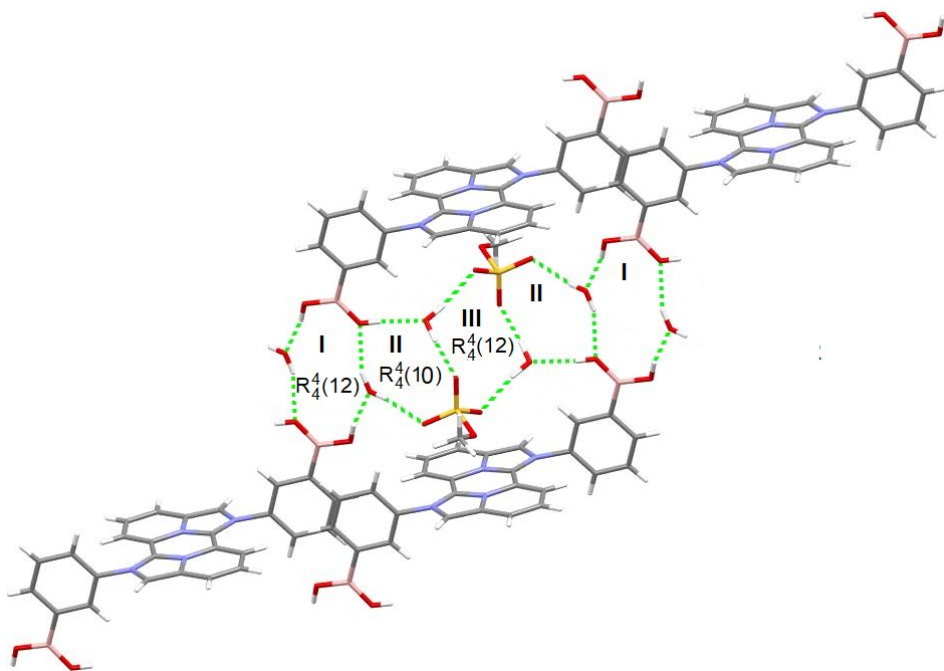


Figure 2. Three different motifs (**I**, **II** and **III**) observed by intermolecular hydrogen bonds interactions in compound **1a**.

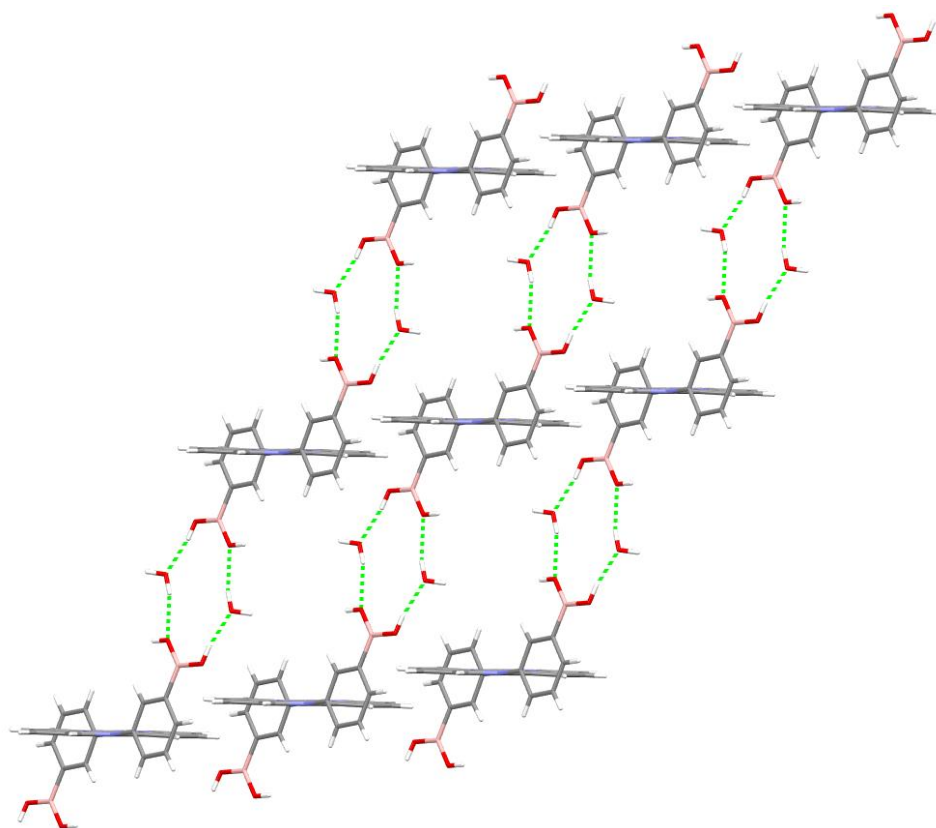
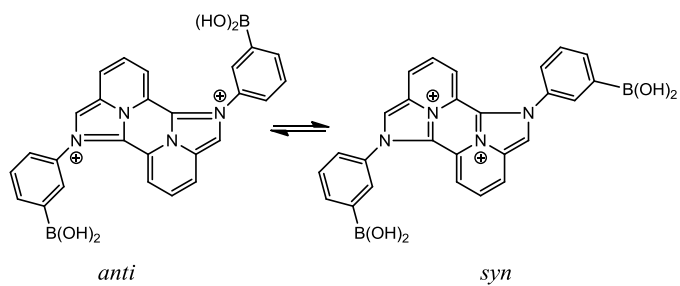


Figure 3. Fragment of supramolecular arrangement supported by O-H \cdots O hydrogen bonds, with water molecules connecting the boronic acid groups in **1a**.



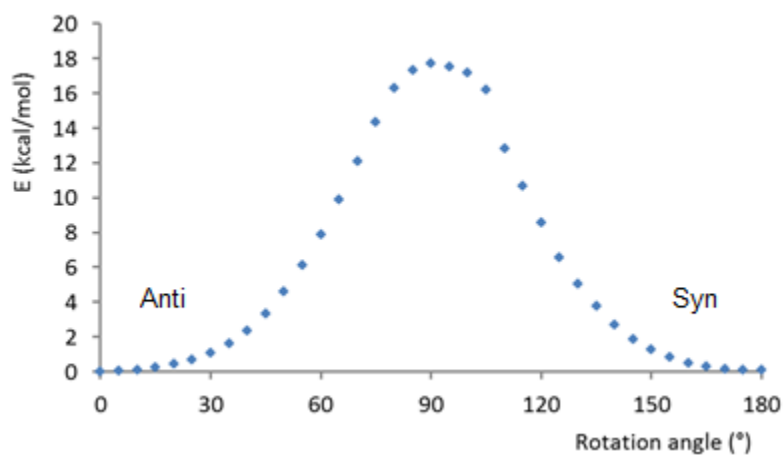


Figure 4. Schematic *anti-syn* equilibrium (top). Energy drawn against rotation angle in the *anti* \rightleftharpoons *syn* isomerization (bottom).

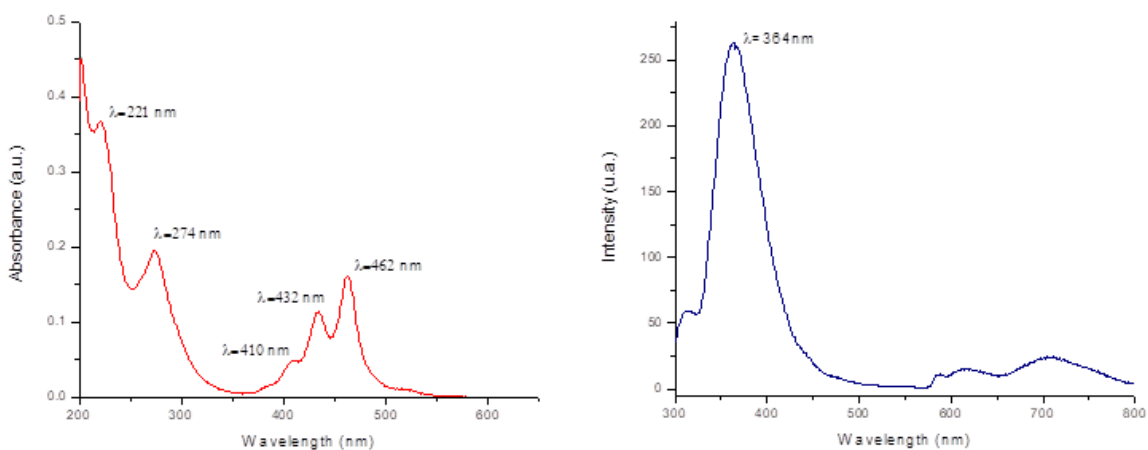


Figure 5. UV-vis and Photoluminescence (excited at 293 nm) spectra for **1a** in methanol solution (10^{-5} M).

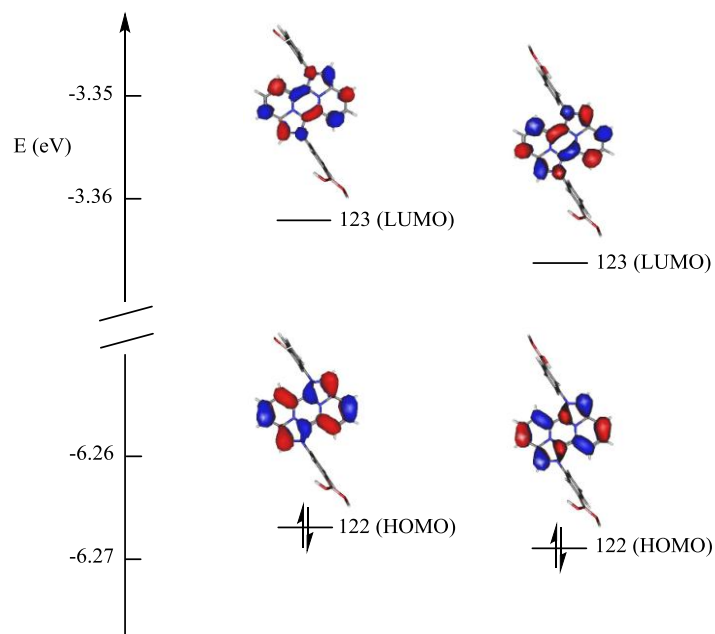


Figure 6. HOMO and LUMO level for the *anti*-(left) and *syn*-(right) isomers.

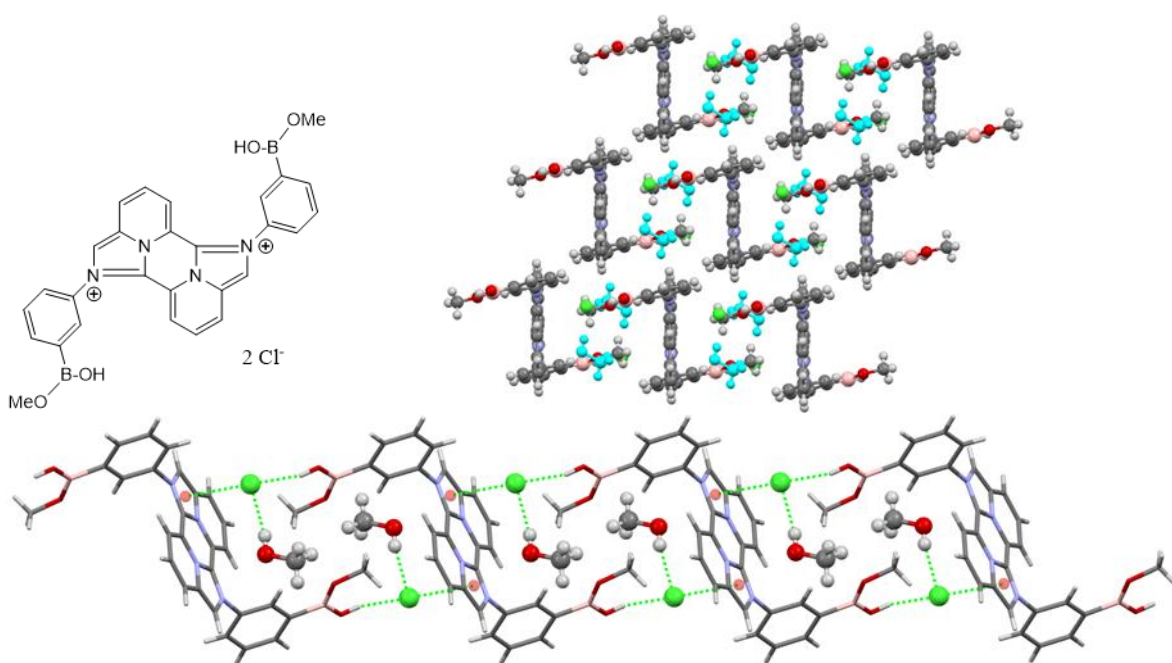


Figure 7. Schematic representation of **1b** (up, left), part of the unit cell showing the sig-zag conformation of **1b** (up, right), and 1D polymeric chain formed by B-OH \cdots Cl, MeO-H \cdots Cl and electrostatic $\pi_{\text{ring}}(+)\cdots\text{Cl}(-)$ interactions (down).

Table 1. Selected Crystallographic data for compounds **1a** and **1b**

<i>Compound</i>	<i>1a</i>	<i>1b</i>
<i>Empirical formula</i>	C ₁₄ H ₁₇ BN ₂ O ₈ S	C ₁₅ H ₁₆ BCIN ₂ O ₃
<i>Formula weight</i>	384.16	318.56
<i>Temperature/K</i>	99.98(18)	99.9(4)
<i>Crystal system</i>	triclinic	triclinic
<i>Space group</i>	P-1	P-1
<i>a/Å</i>	8.1728(4)	7.6948(3)
<i>b/Å</i>	9.5418(4)	8.9781(3)
<i>c/Å</i>	11.8981(7)	11.8347(5)
<i>α/°</i>	109.300(5)	75.820(3)
<i>β/°</i>	96.760(5)	76.513(4)
<i>γ/°</i>	99.797(4)	85.531(3)
<i>Volume/Å³</i>	847.71(8)	770.63(5)
<i>Z</i>	2	2
<i>ρ_{calc}/g/cm³</i>	1.505	1.373
<i>μ/mm⁻¹</i>	2.137	2.309
<i>F(000)</i>	400.0	332.0
<i>Crystal size/mm³</i>	0.36 × 0.28 × 0.14	0.15 × 0.125 × 0.1
<i>Radiation</i>	CuKα (λ = 1.54184)	CuKα (λ = 1.54184)
<i>2θ range for data collection/°</i>	10.076 to 145.216	7.902 to 145.542
<i>Reflections collected</i>	5411	4805
<i>Independent reflections</i>	3276 [R _{int} = 0.0176, R _{sigma} = 0.0292]	2982 [R _{int} = 0.0167, R _{sigma} = 0.0288]
<i>Data/restraints/parameters</i>	3276/0/294	2982/0/203
<i>Goodness-of-fit on F²</i>	1.054	1.076
<i>Final R indexes [I ≥ 2σ (I)]</i>	R1 = 0.0399, wR2 = 0.1074	R1 = 0.0519, wR2 = 0.1485
<i>Final R indexes [all data]</i>	R ₁ = 0.0428, wR ₂ = 0.1101	R ₁ = 0.0551, wR ₂ = 0.1520

Table 2: Selected bond distances (Å), angles and torsion angles (°) for **1a** and **1b**.

	1a	1b
	<i>Torsion Angles (°)</i>	
C13-N1-C3-C2	80.93	74.93
C7-N1-C3-C4	88.71	80.33
O2-B1-C1-C2	4.64	3.51
O1-B1-C1-C6	4.54	2.45
	<i>Bond Angles (°)</i>	
C13-N1-C3	125.06	124.06
C7-N1-C3	124.53	125.49
C13-N1-C7	110.02	110.40
O2-B1-O1	119.40	126.90
O2-B1-C1	123.54	115.12
O1-B1-C1	117.05	117.96
	<i>Bond Distances (Å)</i>	
C13-N1	1.343	1.351
C7-N1	1.371	1.366
C3-N1	1.453	1.447
O1-B1	1.359	1.356
O2-B1	1.356	1.353
C1-B1	1.586	1.587

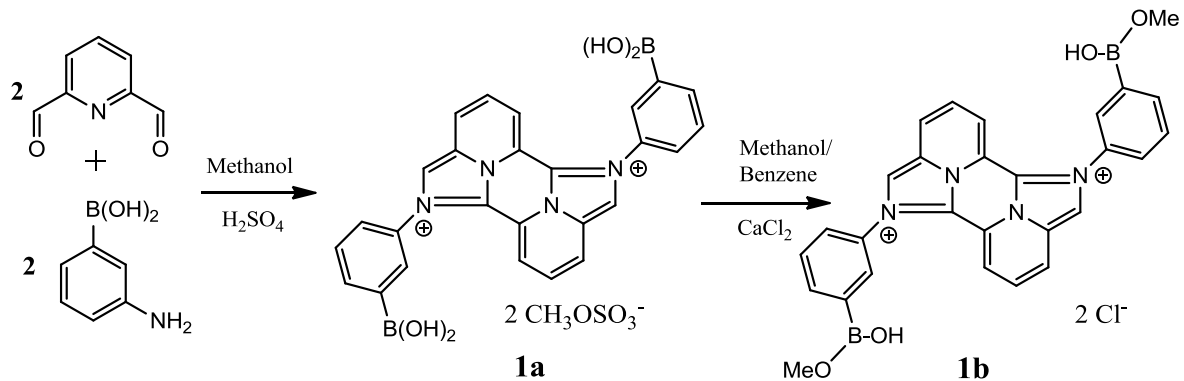
Table 3. Comparison of DFT computed data and experimental (UV-vis) data with absorption maxima (λ_{max} in nm), oscillator strength (f), and extinction coefficient (ε in $\text{mol}^{-1} \text{L cm}^{-1}$) for **1a**.

Transition	DFT computational data		UV-vis experimental data	
	λ_{max}	f	λ_{max}	ε
<i>anti</i>				
1→3	485	0.570	462	19 100
<i>syn</i>				
1→3	459	0.360	432	13 600

Table 4. Dominant transition with absorption maximum (λ_{max}), intensity (oscillator strength f), and composition of the configuration interaction expansion for the *anti*- and the *syn*- isomers, compared with the experimental data

Transition	λ_{max}	f	composition*
<i>anti</i>			
1 \rightarrow 3	485 nm	0.570	98.8 % $\chi_{122\rightarrow 123}$
<i>syn</i>			
1 \rightarrow 3	459 nm	0.360	97.2 % $\chi_{122\rightarrow 123}$

*Orbital 122 (123) is the HOMO (LUMO) in both cases.



An unexpected double condensation reaction between 3-aminophenylboronic acid monohydrate and 2,6-pyridinedicarboxaldehyde offers the fluorescent bisboronic dicationic acid (**1a**), the anion exchange and partial esterification were observable (**1b**) after treatment with CaCl_2 in a benzene/methanol solution.